

Efficient and reversible CO2 capture in bio-based ionic liquids solutions

Original

Efficient and reversible CO2 capture in bio-based ionic liquids solutions / Latini, Giulio; Signorile, Matteo; Rosso, Francesca; Fin, Andrea; D'Amora, Marta; Giordani, Silvia; Pirri, Candido; Crocellà, Valentina; Bordiga, Silvia; Bocchini, Sergio. - In: JOURNAL OF CO2 UTILIZATION. - ISSN 2212-9820. - ELETTRONICO. - 55:(2022), p. 101815. [10.1016/j.jcou.2021.101815]

Availability:

This version is available at: 11583/2947884 since: 2021-12-27T18:23:27Z

Publisher:

Elsevier Ltd.

Published

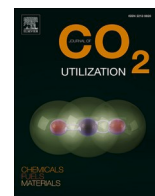
DOI:10.1016/j.jcou.2021.101815

Terms of use:

This article is made available under terms and conditions as specified in the corresponding bibliographic description in the repository

Publisher copyright

(Article begins on next page)



Efficient and reversible CO₂ capture in bio-based ionic liquids solutions

Giulio Latini^{a,b,e}, Matteo Signorile^b, Francesca Rosso^b, Andrea Fin^c, Marta d'Amora^e,
Silvia Giordani^{d,e}, Fabrizio Pirri^{a,e}, Valentina Crocellà^{b,*}, Silvia Bordiga^b, Sergio Bocchini^{e,*}

^a Department of Applied Science and Technology, Politecnico di Torino, Corso Duca degli Abruzzi 24, 10129, Turin, Italy

^b Department of Chemistry, NIS and INSTM Centers, Università di Torino, via G. Quarello 15 and via P. Giuria 7, 10125, Turin, Italy

^c Department of Drug Science and Technology, Università di Torino, via P. Giuria 9, 10125, Turin, Italy

^d School of Chemical Sciences, Dublin City University (DCU), Glasnevin, D09 C7F8, Dublin, Ireland

^e Center for Sustainable Future Technologies, Istituto Italiano di Tecnologia, via Livorno 60, 10144, Torino, Italy

ARTICLE INFO

Keywords:

CO₂ capture
Ionic liquids
Amino-acids
In-situ ATR-IR spectroscopy
In vivo toxicity assessment

ABSTRACT

Choline/amino acid-based ionic liquids were synthesized via ionic metathesis and their CO₂ absorption performances evaluated by employing different experimental approaches. In order to overcome any viscosity-related problem, dimethyl sulfoxide (DMSO) was employed as solvent. IL-DMSO solutions with different IL concentrations were evaluated as absorbents for CO₂, also investigating their good cyclability as desirable for real industrial CO₂ capture technologies. ¹H-NMR and *in-situ* ATR-IR experiments were the toolbox to study the CO₂ chemical fixation mechanism under different experimental conditions, proving the formation of distinct chemical species (carbamic acid and/or ammonium carbamate). In general, these ILs demonstrated molar uptakes higher than classical 0.5 mol CO₂/mol IL and the capacity to release CO₂ in extremely mild conditions. The possible biological adverse effects were also analyzed, for the first time, in zebrafish (*Danio rerio*) during the development, by assessing for different toxicological endpoints, proving the non-toxicity and high biocompatibility of these bio-inspired ILs.

1. Introduction

The atmospheric concentration of carbon dioxide (CO₂) has increased due to the anthropogenic contribution overstepped 400 ppm in 2015 [1,2]. Fossil fuel combustion for energy production, transportation and industrial processes establishes the main contribution to human emission. Purification of post-combustion gases, storage and conversion/utilization of CO₂ represent a straightforward measure to reduce anthropogenic emissions.

Different CO₂ separation techniques are available based on different physico-chemical phenomena: absorption or adsorption, either physical or chemical, membrane or cryogenic-based separation. Besides the working principle, energy consumption, toxicity and operating cost must be taken into account for the technologic implementation [3]. Amine scrubbing process is the most notable and widespread technology: the first process was patented in 1930 [4]. Alkylamine aqueous solutions chemically fix the CO₂ molecule, as shown in Scheme 1. Primary and secondary amines produce ammonium-carbamate species,

whereas ammonium-carbonate species are formed from tertiary amine and water (see Scheme 1) [5–7]. After the capture, the amine solution is regenerated at 100–120 °C via water evaporation and the released CO₂ is compressed to 100–150 bar for sequestration and transportation [8].

The CO₂ release from amine aqueous solutions requires solvent evaporation/condensation, an intensive energy demanding process. Moreover, amine scrubbing has several drawbacks related to the toxicity and the corrosiveness of the sorbent phase. Solving these issues would positively affect both the environmental and the economic impact of the CO₂ capture procedure. Indeed, a lower energy consumption reduces the operational costs and carbon footprint of the entire process, as well as non-corrosive, non-toxic materials are more suitable from the environmental and plant safety point of view.

Ionic liquids (ILs), usually defined as salts with melting temperature lower than 100 °C [9,10], are emerging as promising candidates for CO₂ capture and conversion [11–14]. ILs can solve some critical issues of amine-based aqueous systems, as they feature negligible vapor pressure, non-corrosiveness and high thermal stability [15–19]. Beyond physical

* Corresponding authors at: Center for Sustainable Future Technologies, Istituto Italiano di Tecnologia, via Livorno 60, 10144, Torino, Italy and Department of Chemistry, NIS and INSTM Centers, Università di Torino, via G. Quarello 15 and via P. Giuria 7, 10125, Turin, Italy.

E-mail addresses: valentina.crocella@unito.it (V. Crocellà), sergio.bocchini@iit.it (S. Bocchini).

<https://doi.org/10.1016/j.jcou.2021.101815>

Received 14 July 2021; Received in revised form 24 October 2021; Accepted 18 November 2021

Available online 29 November 2021

2212-9820/© 2021 The Author(s). Published by Elsevier Ltd. This is an open access article under the CC BY license (<http://creativecommons.org/licenses/by/4.0/>).



Scheme 1. Chemical reaction of CO₂ with: (a) a primary/secondary amine; or (b) a tertiary amine in the presence of water.

absorption (which becomes relevant at high pressure), the ILs affinity towards CO₂ can be increased by chemically functionalizing the anion and/or the cation, *i.e.* by introducing an amine group or other basic moieties [20]. Amine-based and amino-tethered ILs capture CO₂ more efficiently through the formation of carbamate species, with a ILs:CO₂ 2:1 stoichiometry [20,21], thus also activating the molecule and opening the path for further reactivity [22,23]. Nonetheless, despite the epithet of “green solvent” [24], ILs commonly tested for CO₂ capture are based on imidazolium and pyridinium cations and fluorinated anions, that hamper their biodegradability and biocompatibility [25,26]. In a green perspective, the choice of non-toxic and biocompatible cations/anions represents a key step to develop a sustainable CO₂ capture process based on ILs. In this scenario, the combination of choline (Cho), a non-toxic, essential nutrient cation, and amino acids (AAs, proteins building block, in the anionic form) could drive to the synthesis of an environmental-friendly class of ILs. In particular, AAs are very convenient anions for a CO₂ capture application, owing to the coexistence of an amine moiety (*i.e.* a specific interaction site for CO₂) and of a carboxylic anion (that enhances the affinity with the sorptive) [27–29], as practically demonstrated by some literature works. Zou et al. tested the capture performance of a choline proline - polyethylene glycol 200 ([Cho][Pro]-PEG200) system at a pressure of 1.1 bar, yielding to a 0.6 CO₂-IL molar ratio [30]. Lu and co-workers studied aqueous solution of choline glycinate, alaninate and proline up to 15 bar of CO₂, obtaining CO₂-IL molar ratios up to 2 and conversion of the carbamate to carbonate, due to the presence of water as solvent and the high pressure involved [31]. More recently, our group revealed closely equimolar CO₂ absorption capacity by some AAs -based ILs (synthesized using Choline as cation and glycine or proline as anions) in dimethyl sulfoxide (DMSO) solution, also investigating the role of the IL concentration on the capture performances [32]. Furthermore, materials based on Cho and AAs (in principle achievable from renewable feedstock) [33,34] have demonstrated good biocompatibility and biodegradability [35–38].

Despite the interesting physico-chemical [39–41] and toxicological [35–38] properties, the employment of these ILs have not spread yet. A first limitation to their employment is the use of choline hydroxide in the usual synthetic procedure. This precursor is expensive, dangerous (it is a corrosive strong base) and difficult to handle. The titration synthesis of neutral AAs by choline hydroxide provides high yields (>90 %) at long reaction times [35–38], involving the aforementioned chemical threats. These factors limit the scalability of this synthetic strategy. In a recent study, we overcome this issue by applying a synthetic approach based on ionic metathesis, suitable for producing higher amounts of choline-based AAILs with a safer procedure [32,42]. The only drawback is the lower purity of the final product due to the presence of halide salts as impurities (< 5 wt% of KCl). However, regarding the application of these ILs in CO₂ capture, this contamination does not seem to affect their performances [32]. Another general drawback of ILs is their high viscosity, which, unfortunately, further increases upon CO₂ interaction [43]. An excessive viscosity prevents gas diffusion into the liquid, negatively affecting the overall capture performances. As a solution, the dilution with proper solvents decreases the viscosity and, at the same time, can also improve the overall absorption capacity thanks to possible solvent-IL synergy and enhanced transport properties [13,14].

In the present work, six different choline-based AAILs, [Cho][AA] ILs, were synthesized *via* ionic metathesis and their CO₂ absorption capacity evaluated by a multi-technique approach in order to evaluate if the presence of different functional groups in the AA anion affects the

CO₂ capture performance. To overcome any viscosity-related issue, dimethyl sulfoxide (DMSO) was selected as solvent, thanks to its high boiling point (189 °C) and its polar and aprotic character. IL-DMSO solutions with different IL concentrations were evaluated as absorbents for CO₂ (also investigating their cyclability). The effective CO₂ chemical fixation was proved by ¹H-NMR and *in-situ* ATR-IR experiments. Furthermore, potential *in vivo* developmental toxicity induced by one of the synthesized ILs has been evaluated on zebrafish (*Dario rerio*), as emerging vertebrate *in vivo* models for nanotoxicity screening, to stress the biocompatibility of this new class of ILs [44–47]. Here, the effects of this ionic liquid were analysed for different toxicological endpoints, including cardiac toxicity, behavioral and possible growth perturbations in zebrafish embryos/larvae. Notably, [Cho][AA] ILs were found to be non-toxic and IL solutions in DMSO demonstrated a molar uptake >0.5 mol CO₂/mol IL and the capacity to release CO₂ in mild condition, *i.e.* avoiding the solvent evaporation.

2. Experimental

2.1. Materials and syntheses

The ILs were prepared by ionic metathesis and purified as previously reported and described in detail in the Supporting Information (Section S1 and Scheme S1) [32,42]. The employed amino acids are glycine, alanine, serine, proline, phenylalanine and sarcosine and the corresponding choline [Cho][AA] ILs are choline glycinate ([Cho][Gly]), choline alaninate ([Cho][Ala]), choline serinate ([Cho][Ser]), choline proline ([Cho][Pro]), choline phenylalaninate ([Cho][Phe]) and choline sarcosinate ([Cho][Sar]) respectively, whose structures are shown in Scheme 2.

The syntheses were confirmed by means of ATR-IR (Fig. S1 and Table S1) and ¹H-NMR (Figs. 3, S2 and Table S2) spectroscopies. The residual KCl content (usually lower than 3 wt%) was evaluated by TG analysis (Fig. S3 and Table S3). AA salts were also prepared as reference materials, as described in Section S1 of Supporting Information. When needed, [Cho][AA] ILs were dissolved in DMSO (supplied by Merck, purity ≥ 99 %) with different concentration. Solutions were prepared as follows: the IL was weighted in a glass vial, and then the DMSO was added, by adjusting its quantity in order to obtain the desired concentration. About 5 g of solution were produced for each concentration. Viscosities and gravimetric densities of AAILs and their DMSO solutions were assessed and listed in Table S4.

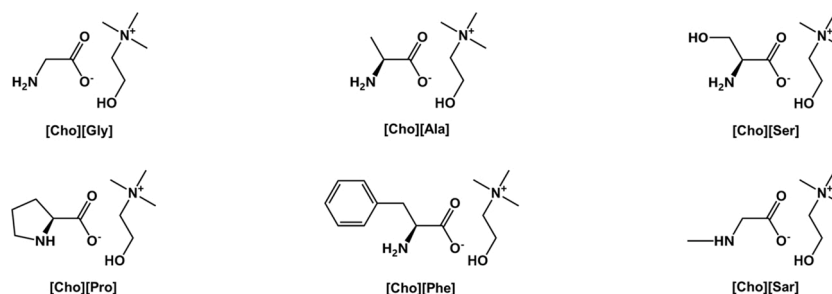
3. Instrumental methods

3.1. CO₂ absorption

The absorption properties of the DMSO-IL systems were evaluated by means of two different experimental setups. A gravimetric approach was employed to measure the CO₂ capacity, whereas multiple absorption/desorption cycles were studied in a custom-made batch reactor with an IR CO₂ sensor to obtain information about the regenerability of the systems.

3.1.1. Gravimetric measurements

The CO₂ absorption was quantified using a gravimetric method. Different IL dilution in DMSO were tested: 50, 33, 20 and 12.5 wt%. Approximately 3 mL of solution were poured in a batch reactor (~4.5 mL), purged for 10 min with N₂ (30 mL/min) and weighted. Then, CO₂ (30 mL/min) was bubbled until no mass increase was observed. The captured CO₂ was calculated by mass difference before and after CO₂ contact, considering the reactor headspace contribution. Two quantities were calculated: CO₂ loading, defined as percentage of captured CO₂ over the total mass of DMSO-IL solution, and the molar efficiency, defined as the molar ratio between captured CO₂ and the amount of IL. The solvent evaporation was previously evaluated on pure DMSO and



Scheme 2. Molecular structures of the synthesized [Cho][AA] ILs and their labels.

estimated to be lower than the balance sensitivity. The error was estimated by propagation starting from instrument sensitivity.

The adsorption capacity of pure ionic liquids has not been evaluated due to their high viscosity, which further increases when they react with CO₂ (until gel and foam formation), hampering the CO₂ diffusion into the bulk liquid phase. The first preliminary tests pointed out a negligible increase in weight also due to the loss of IL stripped by the gas flow.

3.1.2. Adsorption/desorption cycles

Multiple absorption and desorption cycles were carried out in a custom-made reactor provided by HEL Group (schematic is reported in Fig. S4). In a typical experiment, ~5 mL of DMSO-IL solution were used, according to the following steps: (i) purging with a N₂ flow (100 mL/min) for 10 min; (ii) absorption with a synthetic flue gas (20 %v CO₂ in N₂ [48] – 100 mL/min) until saturation (inlet and outlet gas stream had the same composition); (iii) desorption in N₂ flow (100 mL/min) increasing the temperature to 80 °C at 10 °C/min (this temperature was kept until all the CO₂ is released, *i.e.* when the CO₂ is no more detected in the outlet gas stream); (iv) cooling in N₂ flow (100 mL/min). Absorption/desorption cycles lasted similarly, approximately ~90 min. The steps from (ii) to (iv) were repeated 10 times.

3.1.3. NMR

¹H-NMR and ¹H-COSY analyses were performed to confirm the molecular structure of the [Cho][AA] ILs in 12.5 wt% solutions with DMSO-d₆. After that, [Cho][AA] ILs solutions were also investigated upon exposure to a pure CO₂ atmosphere (1 h until saturation) directly inside the NMR tube. Measurements were carried out on a JEOL 600 MHz.

3.1.4. IR spectroscopy

Attenuated total reflection infrared spectroscopy (ATR-IR) was employed to characterize pure ILs and to evaluate the interaction between CO₂ and DMSO-IL solutions. Measurements were carried out on a Bruker Invenio R Fourier transform spectrophotometer equipped with a mercury-cadmium-telluride (MCT) cryogenic detector. The spectra were acquired by accumulating the 32 scans (64 for the background spectrum) in 4000 – 600 cm⁻¹ range with a resolution of 2 cm⁻¹.

An *in situ* IR experiment was specifically designed to mimic real operating condition: a synthetic flue gas mixture was employed (20 %v CO₂ in N₂) was adopted, whereas pure N₂ was chosen as inert gas. The interaction between the synthetic flue gas and DMSO-IL solutions was studied by using an Axiom-Hellma TNL 130H multiple reflections ATR cell designed for liquids analysis. The cell is equipped with an AMTIR-1 refractive element and the thermal control was ensured by a recirculating thermostatic bath. The gas composition and flow rates were controlled by means of a modified version of the setup described in ref. [32] (scheme reported in Fig. S5). In a typical experiment, 3 mL of 12.5 wt% IL-DMSO solution were injected in the cell and undergone to (i) purging, (ii) primary CO₂ absorption, (iii) thermal desorption, (iv) cooling and (v) secondary CO₂ absorption. In detail, the solution was: (i) purged with N₂ (100 mL/min) for 10 min to desorb water and other volatile impurities; the temperature was initially set to 25 °C; (ii)

exposed to the synthetic flue gas (50 mL/min) at 25 °C; (iii) purged with N₂ (50 mL/min) while increasing the temperature to 80 °C with a 1 °C/min rate; (iv) cooled down to 25 °C under N₂ flow (20 mL/min); and (v) re-exposed to the synthetic flue gas (50 mL/min) for a second absorption step. Spectra were acquired continuously across each step.

3.2. In vivo toxicity assessment

3.2.1. Zebrafish maintenance

Adult zebrafish were maintained as previously reported [49]. Briefly, zebrafish were kept at 14h:10 h light-dark cycle and a temperature of 28 °C and were fed three times a day.

3.2.2. Developmental toxicity evaluation of ILs

Embryos at 4 h post-fertilization (hpf) were selected and placed in 24 well-culture plates in the medium [50]. Embryos were incubated at 26 ± 1 °C with four concentrations of [Cho][Ser] aqueous IL test solutions (10, 50, 100, and 200 ppm), and medium as a negative control. Survival and hatching rates were measured daily, while the frequency of movements and the heartbeat rate were calculated in zebrafish larvae at 72 hpf. All the analyses were performed by using a stereomicroscope equipped with a CCD camera. All the experiments were done in triplicates. All animal experiments were performed in full compliance with the revised directive 2010/63/EU.

3.2.3. Statistical analysis

All data were presented as mean ± S.D. Differences among the treatments were analysed by one-way analysis of variance (ANOVA) in combination with Holm-Sidak post hoc. A difference between the treated and the control group was considered to be statistically significant at *p* < 0.01.

4. Results and discussion

4.1. CO₂ absorption capacity

The CO₂ absorption capacity of all [Cho][AA] ILs was assessed in DMSO solution at different concentration, by means of a gravimetric setup (described in detail in the experimental section). Tests were performed by bubbling pure CO₂ (1 atm) directly inside the solutions until saturation. The results (reported in Fig. 1 and in detail in Table S5) were similar for all the amino acids tested as IL anions, however all the [Cho][AA]-DMSO solutions exhibited absorption performances significantly higher compared to literature data of pure DMSO (which report values of about 0.5 wt% at 1 atm) [51]. It is worth noting that by decreasing the IL concentration in DMSO, the solution absorption capacity decreases, whereas the molar efficiency increases. This behavior is in line with previous results reported for [Cho][Gly]-DMSO and [Cho][Pro]-DMSO solutions [32]. Indeed, the higher distance of the ionic couples in less concentrated solutions affects the absorption mechanism, favoring the formation of carbamic acid and, at the same time, hindering the proton transfer involved in the ammonium-carbamate generation.

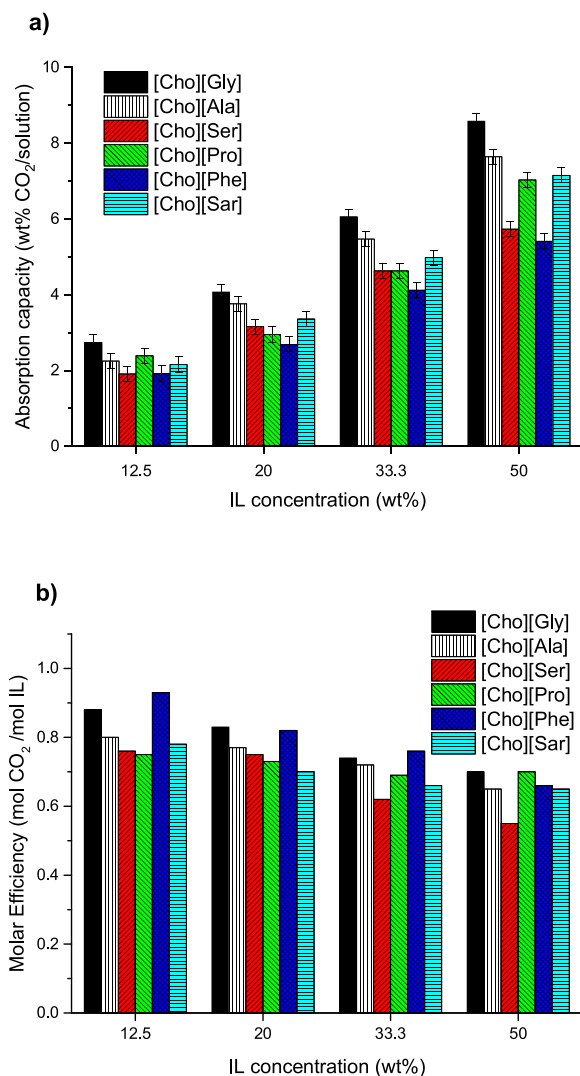


Fig. 1. CO₂ absorption data of [Cho][AA] ILs at different dilutions in DMSO. Panel (a): CO₂ uptake. Panel (b): molar efficiencies.

In general, the various ILs exhibit not so different molar efficiencies (Fig. 1, part b), whereas [Cho][Gly] and [Cho][Phe] possess the highest and the lowest absorption capacities at any concentration, respectively (Fig. 1, part a). Similarly to what previously observed for [Cho][Gly] [32], a solid precipitate forms in [Cho][Ala] solutions during the CO₂ capture process, already in the early stages of the experiment. The precipitate revealed to be solid alanine as testified by the ATR-IR spectra collected on the solid formed during the CO₂ absorption and not reported for the sake of brevity. Being irreversibly degraded during the first absorption cycle, [Gly] and [Ala] containing ILs were not tested in the following cyclic measurements.

Table 1 reports the absorption capacities obtained in the present work (at 50 wt% of IL in DMSO), compared with results obtained with other ILs. Both traditional and [Cho][AA] ILs are reported for completeness. It is worth noting that the significant difference between [bmim][BF₄] (AC = 0.26 and ME = 0.0133) and all the other IL-solvent systems is due to the simple physisorption process occurring in the presence of [bmim][BF₄], compared to the chemisorption of functionalized ILs. Among the functionalized ILs, the absorption capacity (AC) spreads approximately from 4 to 15 wt%, while the molar efficiency (ME) from ~ 0.2 to 0.9 mol/mol. Even though the set of ILs recently studied by Xiong et al. shows notably high absorption capacities, our samples have significantly higher MEs and, at the same time, the great

Table 1

CO₂ absorption capacity (AC, g(CO₂)/g(IL) wt% and g(CO₂)/g(solution) wt%), and molar efficiency (ME, mol(CO₂)/mol(IL)) for different ILs. Presence of solvent, concentration (wt%), temperature (°C) and pressure (bar) employed are reported in brackets, in the first column. Within each block, ILs are reported in order of increasing ME.

IL	AC	ME	Reference
[bmim][BF ₄] ^a (none, 100, 40, 1)	0.26 (0.26)	0.0133	[52]
[DBUH][1,2,3-triaz] ^a (none, 100, 40, 1)	2.8 (2.8)	0.14	
[DBNH][1,2,3-triaz] ^a (none, 100, 40, 1)	3.4 (3.4)	0.15	[53]
[DBUH][1,2,4-triaz] ^a (none, 100, 40, 1)	5.0 (5.0)	0.25	
[DBNH][1,2,4-triaz] ^a (none, 100, 40, 1)	6.2 (6.2)	0.27	
[E ₁ Py][SCN] ^a (none, 100, 30, 15)	4.3 (4.3)	0.19	
[E ₁ Py][N(CN) ₂] ^a (none, 100, 30, 15)	8.3 (8.3)	0.38	[54]
[E ₁ Py][C(CN) ₃] ^a (none, 100, 30, 15)	9.2 (9.2)	0.48	
[BuNH ₂ PrIM][BF ₄] ^b (none, 100, 25, 1)	7.4 (7.4)	0.5	[20]
[bmin][Pro] ^a (none, 100, 25, 2)	5.6 (5.6)	0.32	
[bmin][Gly] ^a (none, 100, 25, 2)	7.9 (7.9)	0.38	[27]
[bmin][Ala] ^a (none, 100, 25, 2)	7.6 (7.6)	0.39	
[bmin][Arg] ^a (none, 100, 25, 2)	8.8 (8.8)	0.62	
[DBNH][Im] ^a (none, 100, 40, 1)	14.9 (14.9)	0.65	
[DBNH][Py] ^a (none, 100, 40, 1)	14.9 (14.9)	0.65	[55]
[DBUH][Im] ^a (none, 100, 40, 1)	13.6 (13.6)	0.68	
[DBUH][Py] ^a (none, 100, 40, 1)	13.4 (13.4)	0.67	
[Bmmop][OAc] ^a (H ₂ O, 40, 25, 18.8)	7.9 (19.6)	0.65	[29]
[Cho][Lys] ^b (H ₂ O, 50, 22, 1)	19.4 (38.8)	2.2	[56]
[Cho][Pro] ^b (PEG200, 50, 35, 1)	6 (12)	0.61	[30]
[Cho][Gly] ^b (DMSO, 50, 25, 1)	8.6 (17.2)	0.78	
[Cho][Ala] ^b (DMSO, 50, 25, 1)	7.6 (15.3)	0.79	
[Cho][Ser] ^b (DMSO, 50, 25, 1)	5.7 (11.5)	0.61	
[Cho][Pro] ^b (DMSO, 50, 25, 1)	7.0 (14.1)	0.84	This work
[Cho][Phe] ^b (DMSO, 50, 25, 1)	5.4 (10.8)	0.70	
[Cho][Sar] ^b (DMSO, 50, 25, 1)	7.2 (14.3)	0.71	

^a Apparatus: CO₂ atmosphere on the absorbent.

^b Apparatus: CO₂ stream.

advantage of good biocompatibility.

The 12.5 wt% concentration, exhibiting a slightly higher molar efficiency in previous gravimetric analyses (Fig. 1), was selected to test the cyclability of all [Cho][AA] ILs aiming to assess the feasibility of cyclic absorption/desorption in a demonstrator unit, simulating the experimental conditions of an industrial CO₂ capture technology. In this experimental setup, the adsorption capacity reflects the absorption and desorption rates of the IL solutions, rather than the real thermodynamic equilibrium, as in the gravimetric measurements. As reported in Fig. 2 (left axis), all [Cho][AA] ILs (and especially [Cho][Phe] and [Cho][Sar]) possess the highest CO₂ absorption capacity during the first cycle, then

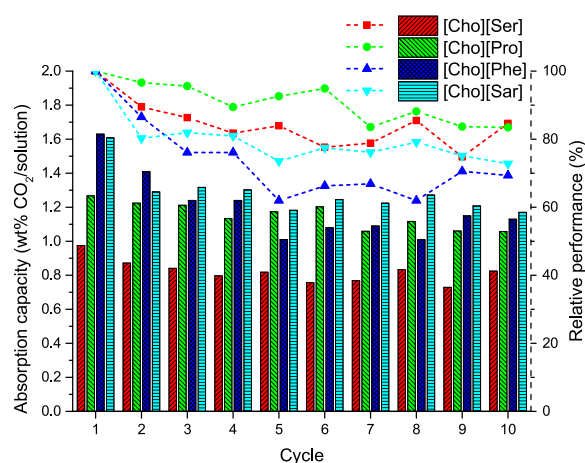


Fig. 2. Cyclic CO₂ absorption measurements over 10 absorption/desorption cycles. Left axis refers to the bars graphs reporting the CO₂ absorption capacity in wt% (w(CO₂)/w(solution)). Right axis refers to the relative performance (%) as the ratio between the absorbed CO₂ in the *i*th cycle and the absorbed CO₂ in the first cycle.

the CO₂ loading gradually decreases along the other absorption/desorption cycles. The CO₂ uptakes are definitely lower if compared to the results obtained for the same IL concentration in the gravimetric measurements of Fig. 1a, due to the lower partial pressure of CO₂ employed in the cyclic experiments. The data of CO₂ uptake highlight that [Cho][Phe] and [Cho][Sar] ILs are the most performing at this concentration and that their absorption capacities suddenly decrease, being soon comparable to the values computed for the [Cho][Pro] solution. In contrast, [Cho][Ser] solution exhibits the lowest values of CO₂ loading. Considering instead the relative performance data of Fig. 2 (right axis) we observe that: (i) the [Cho][Phe] solution, with the highest absorption capacity, possesses the lowest stability along cycles, with an average relative performance of around 65 %; (ii) [Cho][Ser] and [Cho][Sar] solutions have a medium stability, exhibiting relative performances of 75 % during the last three absorption/desorption cycles; (iii) the [Cho][Pro] solution shows the highest relative performance during the last cycles (around 85 %), despite its lower CO₂ uptake, being in some way the best compromise between the capacity to capture CO₂ and the stability along the absorption cycles.

It is worth highlighting that the IL containing the phenyl moiety exhibits the best absorption performances during the first cycle, but its absorption capacity decreases more during the cycles. In contrast, the IL containing a heterocyclic moiety with a secondary amine ([Cho][Pro]) possesses a lower absorption capacity, but it clearly maintains its capture performance during the cyclic experiments. Instead, the presence of a secondary amine inserted in a linear aliphatic chain does not seem affecting the capture performance and stability of [Cho][Sar].

In general, we can conclude that a direct comparison of the cyclic experiments with the gravimetric results is not straightforward, being the CO₂ absorption/desorption equilibria affected by different parameters, among which the IL concentration, the viscosity changes, the surface tension and the CO₂ diffusivity in the solution [57].

4.2. Assessment of the absorption mechanism

The CO₂ absorption process into a bulk [Cho][AA] IL is associated with a real chemical reactivity occurring between the CO₂ molecule and the amine group of the amino acid anion. Therefore, beside the evaluation of the absorption capacities of the DMSO-IL systems, we also investigated their interaction mechanism with CO₂ at a molecular level by means of ¹H-NMR and *in situ* ATR-IR spectroscopies.

4.3. NMR spectroscopy

In ¹H-NMR spectra collected upon interaction of the ILs/DMSO-d₆ solutions with CO₂ (in similar conditions to those adopted in the gravimetric absorption measurements, *i.e.* employing a pure CO₂ stream), the formation of carbamate/carbamic acid species was depicted by a remarkable de-shielding of the signals of the α and β protons to the AA amine moiety, as reported for [Cho][Sar] IL and [Cho][Ser] IL in

Fig. 3. These ILs feature a primary and a secondary amine moiety respectively, and are representative for all the other [Cho][AA] ILs. When the [Cho][Ser] solution (12.5 wt%) interacts with pure CO₂, the α proton undergo a downshift from 2.91 ppm to 3.42 ppm, overlapping to the choline signal, while the well-defined β protons in the pending group at 3.33 and 3.27 ppm shifts to 3.56 ppm (Fig. 3a). [Cho][Sar] IL solution exhibits a similar behavior upon CO₂ absorption, both the α protons pattern and the sarcosinate N-Methyl group signal undergo a downshift from 2.77 to 3.56 ppm and from 2.22 to 2.67 ppm respectively (Fig. 3b). The choline signals were not affected by the CO₂ interaction as well as the equimolar [Cho][AA] ILs component ratio based on the signal integration for all the [Cho][AA] ILs (see Figs. 3 and S2).

After CO₂ absorption, the ¹H-NMR pattern suggests the neat prevalence of a unique chemical species with no traces of side products or degradation in the presence of both primary and secondary amine moieties. Considering the previous gravimetric results reporting the reaction with pure CO₂ and a ILs concentration of 12.5 wt%, these results are in perfect agreement with the molar efficiency values close to 1 obtained for [Cho][Gly] and [Cho][Phe] testifying the formation of carbamic acid. Concerning the other ILs, ([Cho][Sar], [Cho][Ala], [Cho][Pro] and [Cho][Ser]) gravimetric analyses show the concurrent formation in small concentrations of other species, such as carbamate or protonated amines. The absence of multiple signals should be substantiated: the identification and quantification by NMR spectroscopy of these species is not straightforward due to their low concentration, high viscosity of the media and potential overlap with peaks proper of the main species before and/or after the CO₂ absorption.

The protons in α to the amine in the reactive AAs are the most indicative to evaluate the presence and the formation of new species. For [Cho][Ser], [Cho][Pro] and [Cho][Sar] these signals end up overlapping to the choline pattern around 3.5 ppm (Figs. 3 and S2) upon CO₂ contact, thus preventing a precise signal integration. Moreover, it is reasonable to speculate a very close chemical shift for the α protons of very similar species like carbamic acid or carbamate derivative of the same AA. Finally, the high viscosity of AAILs causes the broadening of the proton signals which could hamper the identification of very diluted species.

A comprehensive list of ¹H-NMR peaks is reported in Table S2 pointing out a similar behavior for all the [Cho][AA] ILs.

4.4. *In situ* IR spectroscopy

The CO₂ capture and release were monitored by means of *in situ* ATR-IR spectroscopy, under experimental conditions close to the cyclic absorption measurements, in order to identify the chemical species generated by the CO₂ reaction with [Cho][AA] ILs. Room temperature absorption and following desorption at 80 °C were monitored by *in situ* ATR-IR experiments using 12.5 wt% IL-DMSO solutions of all the synthesized [Cho][AA] ILs. Spectra collected before and after CO₂ interaction and after CO₂ desorption at 80 °C are compared in Fig. 4. For the sake of brevity, only the results of [Cho][Ser] and [Cho][Sar]

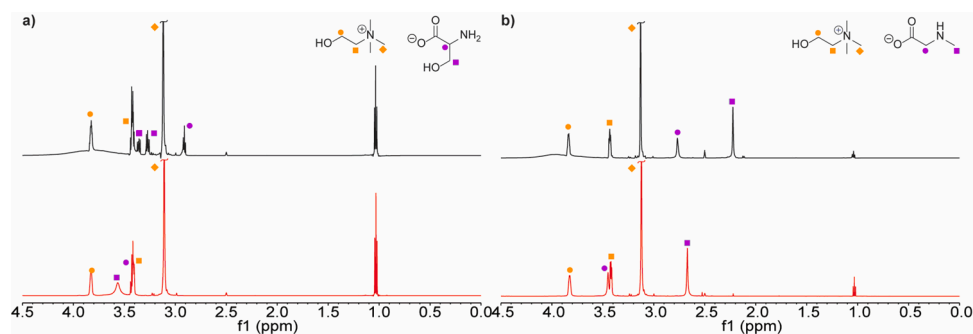


Fig. 3. ¹H-NMR spectra of a) [Cho][Ser] and b) [Cho][Sar] before (black) and after (red) pure CO₂ absorption at atmospheric pressure. Proton signals are labelled for choline (orange) and amino acids (purple).

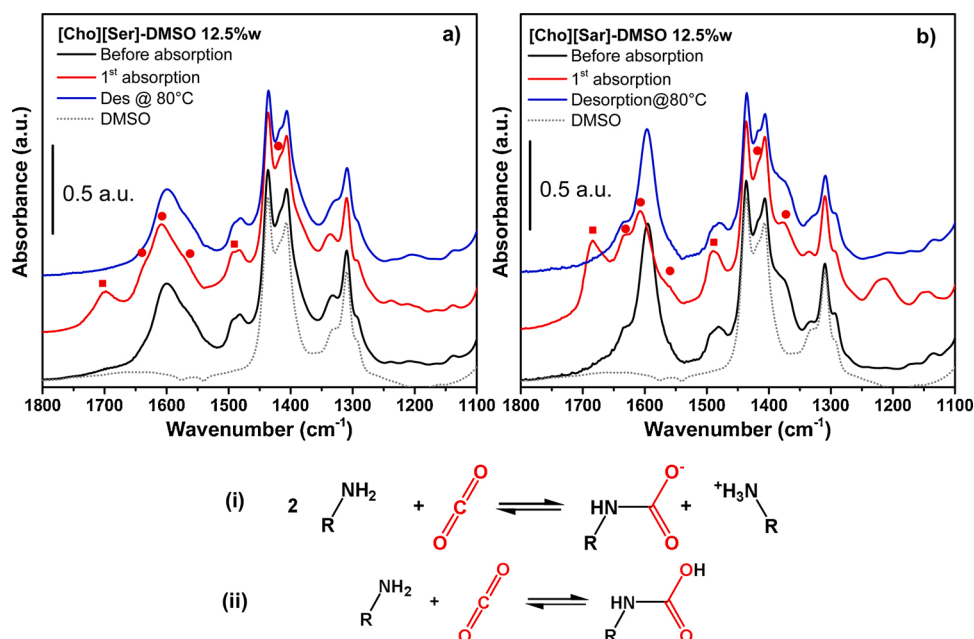


Fig. 4. Upper part: *in situ* ATR-IR spectra in the 1800–1100 cm^{-1} spectral region of (a) [Cho][Ser]-DMSO solution 12.5 wt%; and (b) [Cho][Sar]-DMSO solution 12.5 wt% before CO₂ absorption (black curves), after CO₂ absorption (red curves) and after desorption at 80 °C (blue curves). Dark red circles (●) and squares (■) highlight relevant spectral modifications related to the formation of ammonium carbamate and carbamic acid species, respectively. Lower part: chemical reactions between amines and CO₂ forming (i) ammonium carbamate and (ii) carbamic acid. The spectrum of bare DMSO is reported as reference (grey dotted curve).

(containing a primary or a secondary amine moiety in the AA, respectively) are reported in the main text. The spectra of the remaining ILs are available in Fig. S6 and the detailed summary of the spectral modification generated by the absorption of CO₂ in the different IL-DMSO solutions is reported in Table S6. All reported spectra were collected in different stages of the adsorption/desorption process (as reported in the legend of the figures) after reaching the equilibrium (*i.e.*, when spectral modifications were no more observable).

Spectra of [Cho][Ser]-DMSO 12.5 wt% solution are reported in Fig. 4a. Upon CO₂ absorption (*i.e.* passing from the black to the red curve), different spectral modifications occur. They are related to the reaction paths reported in the lower part of Fig. 4, *i.e.* to the formation of ammonium carbamate (i) and carbamic acid (ii) species, whose IR bands are labelled in Fig. 4 by circles and squares, respectively. In particular, the formation of the ammonium moiety is testified by the appearance in the red spectrum of [Cho][Ser]-DMSO of the shoulder at 1650 cm^{-1} and of the band at 1495 cm^{-1} , ascribed to the asymmetric and the symmetric bending modes of the NH₃⁺ ion. A further confirmation arises from the changes in the vibrational modes of carboxylate species: a +15 cm^{-1} shift of the OCO- asymmetric stretching is indeed evident, suggesting the formation of new carboxylate species (*i.e.*, present in the carbamate moiety). The formation of carbamic acid, instead, is testified by the growth of an intense band at 1700 cm^{-1} , ascribed to the stretching mode of its carbonyl group. All the IL-DMSO solutions containing primary amines (*i.e.*, [Cho][Gly], [Cho][Ala] and [Cho][Phe]) show the same spectral behavior (see Fig. S6).

In contrast, the [Cho][Sar]-DMSO 12.5 wt% solution (see Fig. 4b) spectroscopically behaves in a slightly different way. Indeed, in the presence of [Cho][Sar], the protonation occurs on a secondary amine moiety, giving rise to NH₂⁺ species when the ammonium carbamate forms. The asymmetric and symmetric NH₂⁺ bending modes appear at 1630 and 1490 cm^{-1} , respectively. The formation of ammonium carbamate species is further confirmed by the evolution of the OCO-stretching vibrations: upon CO₂ interaction the asymmetric mode undergoes an upward shift from 1595 to 1610 cm^{-1} while it decreases in intensity, partly overlapping to the signal of protonated amines. The formation of carbamic acid is instead confirmed by the appearance of a peak at around 1700 cm^{-1} , ascribed to the stretching mode of the carbonyl moiety. A similar behavior is observed for [Cho][Pro] (containing an AA with a heterocyclic secondary amine) [32]. In all the [Cho][AA] solutions, the spectra obtained *in situ* after CO₂ desorption by

heating at 80 °C, (see Figs. 4 and S6, blue curves) exhibit a spectral profile very similar to the pristine [Cho][AA] IL. Indeed, all the aforementioned signals disappear, testifying that, during the ATR-IR experiments carried out *in situ*, the CO₂ captured in the form of carbamic acid and ammonium carbamate species is totally released at 80 °C, without any solvent evaporation. *In situ* ATR-IR measurements proved the capacity of CO₂ to effectively react with all the considered amine moieties. In particular, two possible reactions paths were detected: the 1:2 reaction of two amine functional groups (deriving from two distinct IL molecule) with one CO₂ molecule, forming an ammonium carbamate couple (reaction path (i) in Fig. 4), and the 1:1 reaction of a single amine group with one CO₂ molecule, producing carbamic acid (reaction path (ii) in Fig. 4).

The gravimetric absorption measurements proved that the overall [Cho][AA] IL:CO₂ stoichiometry (determined by the molar efficiency) varies according to the [Cho][AA] IL concentration in the DMSO solution. Now, after the spectroscopic identification of two distinct reaction paths, we can infer the IL concentration likely determines the preferred absorption mechanism, occurring *via* the “ammonium carbamate route” in the more concentrated solutions or preferentially through “the carbamic acid route” in the less concentrated ones.

We further checked the cyclability of the absorption process on the [Cho][Ser]-DMSO 12.5 wt% solution by means of *in situ* ATR-IR spectroscopy, by performing a secondary absorption run (always at room temperature), after the primary desorption step at 80 °C. As reported in Fig. S7, spectra collected *in situ* immediately after the first and the second absorption cycle, show negligible differences. This result again highlights the excellent cyclability of these IL-DMSO solutions.

These last results seem to be in contrast with the data of the multiple absorption/desorption cycles collected using the custom-made reactor (to mimic the experimental conditions of a real CO₂ capture technology) and reported in Fig. 2. For this reason, we decided to collect ATR-IR spectra of one of the IL-DMSO solution immediately after the synthesis (fresh) and after ten CO₂ absorption/desorption cycles (used: 10 cycles) in the custom-made reactor, to explain the decrease of the absorption performances observed after several cycles employing this setup. The [Cho][Phe]-DMSO solution was selected due to its more pronounced decrease of the CO₂ absorption capacity during the cyclic tests. Spectra are reported in the Supporting Information (Section S3.3, Fig. S8). Before the ATR-IR measurements, the 10th cycle has been followed by a final desorption step at 80 °C, until CO₂ was no more detected in the

outlet gas stream. It means that, if the absorption process is totally reversible, the spectra collected on fresh sample (black curve) and on the solution after the 10th absorption/desorption cycle (red curve) should coincide. Fig. S8 reports the spectra of the [Cho][Phe]-DMSO solution at the concentration of 12.5 wt% in the 1800-1100 cm⁻¹ spectral range, where the bands generated by the reaction with CO₂ are mainly located. The spectrum collected after 10 cycles (red) does not show any spectral evidence of possible degradation phenomena of the IL and exhibits only the bands generated by the chemical absorption of CO₂. The presence of the signals due to the species generated by the chemical reaction of CO₂ with the IL proves that the specific conditions used in cyclic experiment performed in the custom-made reactor do not allow a complete regeneration of the IL-DMSO solution upon several absorption/desorption cycles. Despite these results, the *in situ* ATR-IR measurements clearly highlighted the great potentiality of these bio-based ionic liquids solutions that can ideally release all the absorbed CO₂ in mild conditions.

4.5. *In vivo* toxicity assessment

To evaluate the developmental toxicity of the [Cho][AA] ILs on zebrafish, we treated the embryos with various concentrations (10, 50, 100, and 200 ppm) of [Cho][Ser] for 120 hpf, and we measured the different toxicological endpoints. The resulting graphs are reported in Fig. 5. In particular, the hatching and survival rates were monitored every 24 h. Following the exposure with IL from 10 ppm up to 200 ppm, the survival rates showed a profile time and concentration-dependent with no relevant decrease during the temporal window analysed (Fig. 5a). At the highest concentration investigated (200 ppm) and after 120 hpf, the value of survival was up to 95%. In addition, the ability to successfully hatch (hatching rates) of the treated groups showed negligible reduction compared to the control group (Fig. 5b). The treated

embryos hatched in the normal temporal window (between 48 and 72 hpf). In fact, at 72 hpf, 95 % of embryos treated with the highest concentration of [Cho][Ser] hatched. In accordance with the OECD guidelines [58], the profiles and trends of the hatching and survival rates of zebrafish treated with [Cho][Ser] indicated that the investigated IL did not have adverse effects on the embryogenesis of zebrafish.

To further investigate the effects of the IL on zebrafish, we measured the heartbeat rates and frequency of movements of treated larvae at 72 hpf. The heartbeat rates of larvae exposed to the [Cho][Ser] showed no significant decrease or increase compared to the control groups (Fig. 5c). Similarly, the frequency of movements of 72 hpf larvae exposed to [Cho][Ser] (Fig. 5d), presented no perturbations in comparison with the control samples. The values of heartbeat rate and frequency of movements indicated that [Cho][Ser] did not influence the cardiac and swimming activities of treated larvae, further confirming that the IL did not affect the embryogenesis.

5. Conclusions

In this work, we presented the complete advanced characterization of different amino acid-based ILs ([Cho][AA] ILs), as such or during their reaction with CO₂. The toxicity of one [Cho][AA] IL was assessed as well, to definitely prove the high bio-compatibility of these systems.

The synthetic method developed was proven to be generally suitable for different AAs, with a minimal content of residual impurity (as such KCl). The interaction between the [Cho][AA] ILs and CO₂ was first tested by means of gravimetric measurements carried out at different dilutions in DMSO. The dependence of the molar efficiency on the concentration of [Cho][AA] ILs in DMSO suggested that different interaction mechanisms could be involved, as already proposed in our previous work [32]. Except for [Cho][Gly] and [Cho][Ala] solutions,

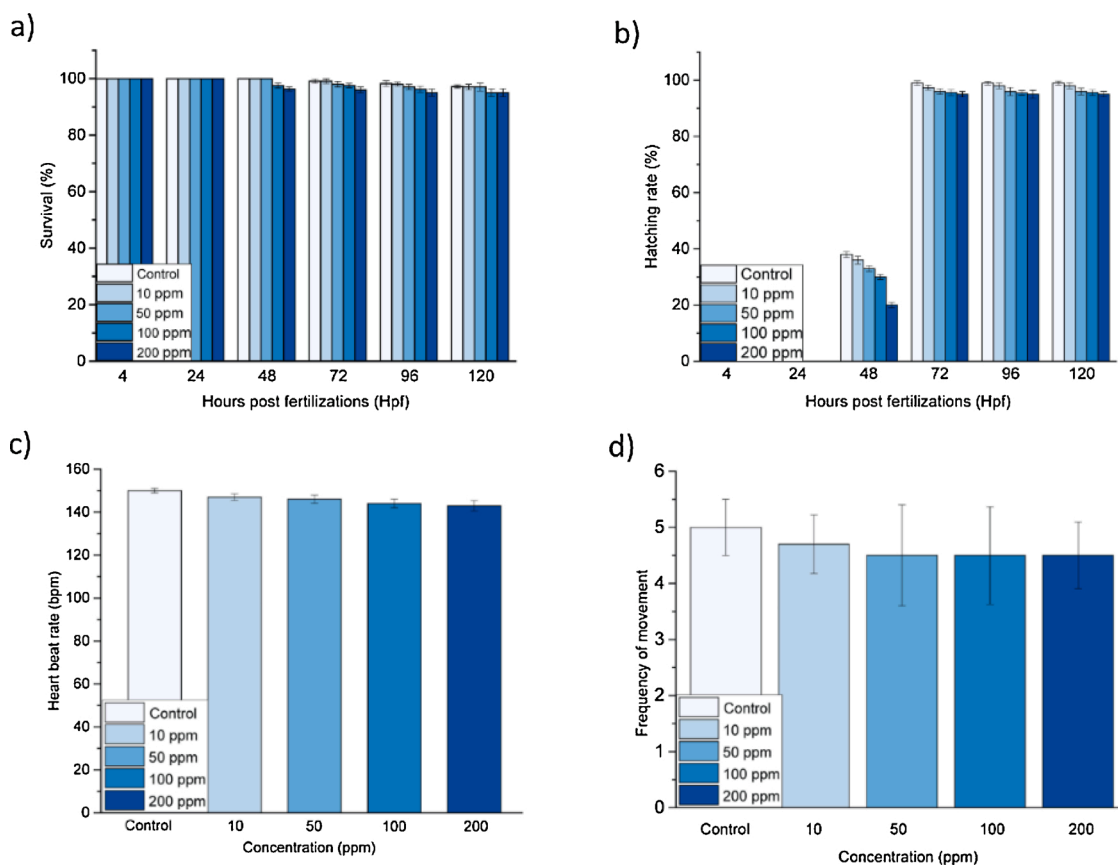


Fig. 5. (a) Survival rate (b) hatching rates, (c) heart beat rate and (d) frequency of movements of zebrafish treated with [Cho][Ser]. Data are calculated as means \pm S. D., from three independent experiments, n = 80; *p \leq 0.1 in comparison to the control.

undergoing AA precipitation upon CO₂ exposure, subsequent cyclic absorption/desorption tests with a custom-made reactor demonstrated the effectiveness of [Cho][AA] IL-DMSO systems in the liquid phase CO₂ capture process, even for several cycles, as desirable for real applications. In particular, the [Cho][Phe] solution possessed the highest CO₂ uptake during the first cycle, but its absorption capacity suddenly decreased in the following cycles. On the other hand, the [Cho][Pro] solution, containing a heterocyclic moiety with a secondary amine, exhibited the highest stability along the absorption cycles, losing just the 15 % of its absorption performance during the first ten cycles. Further studies are needed to really understand the main reason of this peculiar behavior and to explain how the presence of different functionalities in the IL affects the final absorption performances.

The CO₂ capture and release mechanisms were studied in detail by means of ¹H-NMR and *in situ* ATR-IR spectroscopies under different experimental conditions. ¹H-NMR spectroscopy confirmed the neat prevalence of a unique species identified with carbamic acid when the sorbents are exposed to a pure CO₂ stream until saturation. ATR-IR spectroscopy, performed employing a synthetic flue gas stream (*i.e.* in the presence of diluted CO₂) proved the formation of both carbamic acid and ammonium carbamate species, justifying the CO₂: AAIL stoichiometry in the 0.5–1 range observed in the gravimetric experiments. It is evident that the CO₂ relative pressure in the gas stream and the different experimental conditions could be responsible for the preferable absorption pathway giving rise to distinct species (carbamic acid and/or ammonium carbamate). Indeed, the high CO₂ pressure employed in NMR experiments probably promotes the formation of a single product (carbamic acid).

Another important result concerns the CO₂ temperature release of the [Cho][AA] IL-DMSO solutions. Indeed, it is worth noting that, compared to the classical aqueous amine solutions (requiring temperatures higher than 100 °C to achieve a complete CO₂ release), these ILs totally desorb CO₂ at milder conditions (the total release of CO₂ occurs at 70–80 °C, as clearly proved by *in situ* ATR-IR experiments).

Finally, the present study reported, for the first time, the *in vivo* evaluation of the toxicological profile of a [Cho][AA] IL in vertebrate systems, demonstrating the non-toxicity and high biocompatibility of [Cho][Ser] in zebrafish during the development. More in general, the results reported in this work proved how these bio-inspired ILs are very promising alternatives to the classical amine aqueous solutions, mainly thanks to their significantly low CO₂ release temperature, good regenerability and high biocompatibility.

Author statement

Giulio Latini: Conceptualization Methodology Validation Investigation, Data Curation, Writing - Original Draft, Writing - Review & Editing, Visualization. Matteo Signorile: Methodology, Writing - Original Draft, Writing - Review & Editing. Francesca Rosso: Investigation, Writing - Review & Editing. Andrea Fin: Investigation, Resources Writing Original Draft, Writing Review & Editing. Marta d'Amora: Validation, Formal analysis, Investigation, Writing Original Draft, Writing - Review & Editing. Silvia Giordani: Resources, Writing - Review & Editing. Fabrizio Pirri: Resources, Founding acquisition, Supervision. Valentina Crocellà Methodology, Investigation, Writing - Review & Editing, Supervision. Silvia Bordiga: Resources, Writing - Review & Editing, Supervision. Sergio Bocchini: Conceptualization, Methodology, Investigation, Resources, Writing Review & Editing, Supervision, Project Administration.

Declaration of Competing Interest

The authors declare that they have no known competing financial interests or personal relationships that could have appeared to influence the work reported in this paper.

Acknowledgements

We would like to acknowledge Ms. Maria Chiara Lombardi for her contribution to the gravimetric measures and NMR analysis. This project has received funding from the European Union's Horizon 2020 research and innovation program under grant agreement 768583– RECODE (Recycling carbon dioxide in the cement industry to produce added-value additives: a step towards a CO₂ circular economy) project.

Appendix A. Supplementary data

Supplementary material related to this article can be found, in the online version, at doi:<https://doi.org/10.1016/j.jcou.2021.101815>.

References

- [1] Record annual increase of carbon dioxide observed at Mauna Loa for 2015, Science.gov Websites. <https://www.noaa.gov/news/record-annual-increase-of-carbon-dioxide-observed-at-mauna-loa-for-2015>. (Consulted 27 November 2021).
- [2] Vincent Gray, Climate change 2007: the physical science basis summary for policymakers, Energy Environ. 18 (3–4) (2007) 433–440, <https://doi.org/10.1260/095830507781076194>.
- [3] S. Bocchini, et al., The virtuous CO₂ circle or the three cs: Capture, cache, and convert, J. Nanomater. 2017 (2017) 1–14, <https://doi.org/10.1155/2017/6594151>.
- [4] G. Corp, Separating Acid Gases, US1783901, 1930.
- [5] D. Barth, C. Tondre, G. Lappai, J.J. Delpuech, Kinetic study of carbon dioxide reaction with tertiary amines in aqueous solutions, J. Phys. Chem. 85 (November (24)) (1981) 3660–3667, <https://doi.org/10.1021/j150624a027>.
- [6] P.M.M. Blauwhoff, G.F. Versteeg, W.P.M. Van Swaaij, A study on the reaction between CO₂ and alkanolamines in aqueous solutions, Chem. Eng. Sci. 39 (2) (1984) 207–225, [https://doi.org/10.1016/0009-2509\(84\)80021-4](https://doi.org/10.1016/0009-2509(84)80021-4).
- [7] B. Arstad, R. Blom, O. Swang, CO₂ absorption in aqueous solutions of alkanolamines: mechanistic insight from quantum chemical calculations, J. Phys. Chem. A 111 (February (7)) (2007) 1222–1228, <https://doi.org/10.1021/jp065301v>.
- [8] G.T. Rochelle, Amine scrubbing for CO₂ capture, Science (80-) 325 (September (5948)) (2009) 1652–1654, <https://doi.org/10.1126/science.1176731>.
- [9] P. Walden, Ueber die molekulargrosse und elektrische leitfähigkeitteiner gesehmolzenen salze, Bull. Acad. Imper. Sci (St Petersburg) 8 (6) (1914) 405–422.
- [10] N.V. Plechkova, K.R. Seddon, Applications of ionic liquids in the chemical industry, Chem. Soc. Rev. 37 (1) (2008) 123–150, <https://doi.org/10.1039/b006677j>.
- [11] Z.Z. Yang, Y.N. Zhao, L.N. He, CO₂ chemistry: task-specific ionic liquids for CO₂ capture/activation and subsequent conversion, RSC Adv. 1 (4) (2011) 545–567, <https://doi.org/10.1039/c1ra00307k>.
- [12] S. Sarmad, J.P. Mikkola, X. Ji, Carbon dioxide capture with ionic liquids and deep eutectic solvents: a new generation of sorbents, ChemSusChem 10 (January (2)) (2017) 324–352, <https://doi.org/10.1002/cssc.201600987>.
- [13] S. Zeng, et al., Ionic-liquid-based CO₂ capture systems: structure, interaction and process, Chem. Rev. 117 (14) (2017) 9625–9673, <https://doi.org/10.1021/acs.chemrev.7b00072>.
- [14] G. Cui, J. Wang, S. Zhang, Active chemisorption sites in functionalized ionic liquids for carbon capture, Chem. Soc. Rev. 45 (15) (2016) 4307–4339, <https://doi.org/10.1039/c5cs00462d>.
- [15] J.P. Hallett, T. Welton, Room-temperature ionic liquids: solvents for synthesis and catalysis. 2, Chem. Rev. 111 (May (5)) (2011) 3508–3576, <https://doi.org/10.1021/cr1003248>.
- [16] R.D. Rogers, K.R. Seddon, Ionic liquids – solvents of the future? Science (80-) 302 (October (5646)) (2003) 792–793, <https://doi.org/10.1126/science.1090313>.
- [17] H. Olivier-Bourbigou, L. Magna, D. Morvan, Ionic liquids and catalysis: recent progress from knowledge to applications, Appl. Catal. A Gen. 373 (1–2) (2010) 1–56, <https://doi.org/10.1016/j.apcata.2009.10.008>.
- [18] C. Verma, I.B. Obot, I. Bahadur, E.S.M. Sherif, E.E. Ebenso, Choline based ionic liquids as sustainable corrosion inhibitors on mild steel surface in acidic medium: gravimetric, electrochemical, surface morphology, DFT and Monte Carlo simulation studies, Appl. Surf. Sci. 457 (2018) 134–149, <https://doi.org/10.1016/j.apsusc.2018.06.035>.
- [19] C. Verma, E.E. Ebenso, M.A. Quraishi, Corrosion inhibitors for ferrous and non-ferrous metals and alloys in ionic sodium chloride solutions: a review, J. Mol. Liq. 248 (2017) 927–942, <https://doi.org/10.1016/j.molliq.2017.10.094>.
- [20] E.D. Bates, R.D. Mayton, I. Ntai, J.H. Davis, CO₂ capture by a task-specific ionic liquid, J. Am. Chem. Soc. 124 (February (60)) (2002) 926–927, <https://doi.org/10.1021/ja017593d>.
- [21] P. Hu, et al., Absorption performance and mechanism of CO₂ in aqueous solutions of amine-based ionic liquids, Energy Fuels 29 (9) (2015) 6019–6024, <https://doi.org/10.1021/acs.energyfuels.5b01062>.
- [22] Z.Z. Yang, L.N. He, S.Y. Peng, A.H. Liu, Lewis basic ionic liquids-catalyzed synthesis of 5-aryl-2-oxazolidinones from aziridines and CO₂ under solvent-free conditions, Green Chem. 12 (10) (2010) 1850–1854, <https://doi.org/10.1039/c0gc00286k>.

- [23] Z.Z. Yang, L.N. He, C.X. Miao, S. Chanfreau, Lewis basic ionic liquids-catalyzed conversion of carbon dioxide to cyclic carbonates, *Adv. Synth. Catal.* 352 (August (13)) (2010) 2233–2240, <https://doi.org/10.1002/adsc.201000239>.
- [24] M.J. Earle, K.R. Seddon, Ionic liquids. Green solvents for the future, *Pure Appl. Chem.* 72 (January (7)) (2000) 1391–1398, <https://doi.org/10.1351/pac200072071391>.
- [25] K.M. Docherty, C.F. Kulpa, Toxicity and antimicrobial activity of imidazolium and pyridinium ionic liquids, *Green Chem.* 7 (4) (2005) 185–189, <https://doi.org/10.1039/b419172b>.
- [26] R.J. Bernot, M.A. Brueseke, M.A. Evans-White, G.A. Lamberti, Acute and chronic toxicity of imidazolium-based ionic liquids on *Daphnia magna*, *Environ. Toxicol. Chem.* 24 (1) (2005) 87–92, <https://doi.org/10.1897/03-635.1>.
- [27] Y.S. Sista, A. Khanna, CO₂ absorption studies in amino acid-anion based ionic liquids, *Chem. Eng. J.* 273 (August) (2015) 268–276, <https://doi.org/10.1016/j.cej.2014.09.043>.
- [28] N.M. Yunus, N.H. Halim, C.D. Wilfred, T. Murugesan, J.W. Lim, P.L. Show, Thermophysical properties and CO₂ absorption of ammonium-based protic ionic liquids containing acetate and butyrate anions, *Processes* 7 (November (11)) (2019) 820, <https://doi.org/10.3390/pr7110820>.
- [29] C. Ma, S.K. Shukla, R. Samikannu, J.P. Mikkola, X. Ji, CO₂ separation by a series of aqueous morpholinium-based ionic liquids with acetate anions, *ACS Sustain. Chem. Eng.* 8 (January (1)) (2020) 415–426, <https://doi.org/10.1021/acssuschemeng.9b05686>.
- [30] X. Li, et al., Absorption of CO₂ by ionic liquid/polyethylene glycol mixture and the thermodynamic parameters, *Green Chem.* 10 (August (8)) (2008) 879–888, <https://doi.org/10.1039/b801948g>.
- [31] S. Yuan, Y. Chen, X. Ji, Z. Yang, X. Lu, Experimental study of CO₂ absorption in aqueous cholinium-based ionic liquids, *Fluid Phase Equilib.* 445 (2017) 14–24, <https://doi.org/10.1016/j.fluid.2017.04.001>.
- [32] G. Latini, M. Signorile, V. Crocellà, S. Bocchini, C.F. Pirri, S. Bordiga, Unraveling the CO₂ reaction mechanism in bio-based amino-acid ionic liquids by operando ATR-IR spectroscopy, *Catal. Today* 336 (October) (2019) 148–160, <https://doi.org/10.1016/j.cattod.2018.12.050>.
- [33] R.E. Kirk, et al., *Kirk-Othmer Encyclopedia of Chemical Technology*, 4th ed., John Wiley & Sons, Inc, 2000.
- [34] T.M. Lammens, M.C.R. Franssen, E.L. Scott, J.P.M. Sanders, Availability of protein-derived amino acids as feedstock for the production of bio-based chemicals, *Biomass Bioenergy* 44 (September) (2012) 168–181, <https://doi.org/10.1016/j.biombioe.2012.04.021>.
- [35] M. Petkovic, et al., Novel biocompatible cholinium-based ionic liquids toxicity and biodegradability, *Green Chem.* 12 (4) (2010) 643–664, <https://doi.org/10.1039/b922247b>.
- [36] K.D. Weaver, H.J. Kim, J. Sun, D.R. MacFarlane, G.D. Elliott, Cyto-toxicity and biocompatibility of a family of choline phosphate ionic liquids designed for pharmaceutical applications, *Green Chem.* 12 (3) (2010) 507–551, <https://doi.org/10.1039/b918726j>.
- [37] X.D. Hou, Q.P. Liu, T.J. Smith, N. Li, M.H. Zong, Evaluation of toxicity and biodegradability of cholinium amino acids ionic liquids, *PLoS One* 8 (3) (2013), <https://doi.org/10.1371/journal.pone.0059145>.
- [38] W. Gouveia, et al., Toxicity of ionic liquids prepared from biomaterials, *Chemosphere* 104 (2014), <https://doi.org/10.1016/j.chemosphere.2013.10.055>.
- [39] Q.P. Liu, X.D. Hou, N. Li, M.H. Zong, Ionic liquids from renewable biomaterials: synthesis, characterization and application in the pretreatment of biomass, *Green Chem.* 14 (January (2)) (2012) 304–307, <https://doi.org/10.1039/c2gc16128a>.
- [40] S. De Santis, et al., Cholinium-amino acid based ionic liquids: a new method of synthesis and physico-chemical characterization, *Phys. Chem. Chem. Phys.* 17 (32) (2015) 20687–20698, <https://doi.org/10.1039/c5cp01612f>.
- [41] D.J. Tao, Z. Cheng, F.F. Chen, Z.M. Li, N. Hu, X.S. Chen, Synthesis and thermophysical properties of biocompatible cholinium-based amino acid ionic liquids, *J. Chem. Eng. Data* 58 (6) (2013) 1542–1548, <https://doi.org/10.1021/jc301103d>.
- [42] E. Davarpanah, S. Hernández, G. Latini, C.F. Pirri, S. Bocchini, Enhanced CO₂ absorption in organic solutions of bio-based ionic liquids, *Adv. Sustain. Syst.* 4 (December (1)) (2020) 1900067, <https://doi.org/10.1002/adsu.201900067>.
- [43] K.E. Gutowski, E.J. Maginn, Amine-functionalized task-specific ionic liquids: a mechanistic explanation for the dramatic increase in viscosity upon complexation with CO₂ from molecular simulation, *J. Am. Chem. Soc.* 130 (44) (2008) 14690–14704, <https://doi.org/10.1021/ja804654b>.
- [44] M. D'Amora, S. Giordani, The utility of zebrafish as a model for screening developmental neurotoxicity, *Front. Neurosci.* 12 (December) (2018), <https://doi.org/10.3389/fnins.2018.00976>.
- [45] Y.J. Dai, et al., Zebrafish as a model system to study toxicology, *Environ. Toxicol. Chem.* 33 (January (1)) (2014) 11–17, <https://doi.org/10.1002/etc.2406>.
- [46] L. Truong, S.L. Harper, R.L. Tanguay, Evaluation of embryotoxicity using the zebrafish model, in: *Methods in Molecular Biology* (Clifton, N.J.), vol. 691, 2011, pp. 271–279.
- [47] A.J. Hill, H. Teraoka, W. Heideman, R.E. Peterson, Zebrafish as a model vertebrate for investigating chemical toxicity, *Toxicol. Sci.* 86 (July (1)) (2005) 6–19, <https://doi.org/10.1093/toxsci/kfi110>.
- [48] J.G. Vitillo, Magnesium-based systems for carbon dioxide capture, storage and recycling: from leaves to synthetic nanostructured materials, *RSC Adv.* 5 (46) (2015) 36192–36239, <https://doi.org/10.1039/c5ra02835c>.
- [49] M. d'Amora, A. Lamberti, M. Fontana, S. Giordani, Toxicity assessment of laser-induced graphene by zebrafish during development, *J. Phys. Mater.* 3 (June (3)) (2020) 034008, <https://doi.org/10.1088/2515-7639/ab9522>.
- [50] A. Romero, A. Santos, J. Tojo, A. Rodríguez, Toxicity and biodegradability of imidazolium ionic liquids, *J. Hazard. Mater.* 151 (1) (2008) 268–273, <https://doi.org/10.1016/j.jhazmat.2007.10.079>.
- [51] L. Hua, Thermodynamic model of solubility for CO₂ in dimethyl sulfoxide, *Phys. Chem. Liq.* 47 (June (3)) (2009) 296–301, <https://doi.org/10.1080/00319100701788360>.
- [52] J. Jacquemin, M.F. Costa Gomes, P. Husson, V. Majer, Solubility of carbon dioxide, ethane, methane, oxygen, nitrogen, hydrogen, argon, and carbon monoxide in 1-butyl-3-methylimidazolium tetrafluoroborate between temperatures 283K and 343K and at pressures close to atmospheric, *J. Chem. Thermodyn.* 38 (April (4)) (2006) 490–502, <https://doi.org/10.1016/j.jct.2005.07.002>.
- [53] X. Zhang, W. Xiong, Z. Tu, L. Peng, Y. Wu, X. Hu, Supported ionic liquid membranes with dual-site interaction mechanism for efficient separation of CO₂, *ACS Sustain. Chem. Eng.* 7 (June (12)) (2019) 10792–10799, <https://doi.org/10.1021/acssuschemeng.9b01604>.
- [54] S. Hussain, et al., Investigation uncovered the impact of anions on CO₂ absorption by low viscous ether functionalized pyridinium ionic liquids, *J. Mol. Liq.* 336 (August) (2021) 116362, <https://doi.org/10.1016/j.molliq.2021.116362>.
- [55] W. Xiong, M. Shi, L. Peng, X. Zhang, X. Hu, Y. Wu, Low viscosity superbase protic ionic liquids for the highly efficient simultaneous removal of H₂S and CO₂ from CH₄, *Sep. Purif. Technol.* 263 (May) (2021) 118417, <https://doi.org/10.1016/j.seppur.2021.118417>.
- [56] C.F. Martins, et al., Modelling CO₂ absorption in aqueous solutions of cholinium lysinate ionic liquid, *Chem. Eng. J.* 421 (October) (2021) 127875, <https://doi.org/10.1016/j.cej.2020.127875>.
- [57] F. Ortloff, M. Roschitz, M. Ahrens, F. Graf, T. Schubert, T. Kolb, Characterization of functionalized ionic liquids for a new quasi-isothermal chemical biogas upgrading process, *Sep. Purif. Technol.* 195 (April) (2018) 413–430, <https://doi.org/10.1016/j.seppur.2017.12.014>.
- [58] OECD, Test No. 236: Fish Embryo Acute Toxicity (FET) Test, no. July, OECD, 2013.